THE JOURNAL OF BIOLOGICAL CHEMISTRY
Vol. 273, No. 18, Issue of May 1, pp. 11049–11055, 1998
Printed in U.S.A.

Acyl Coenzyme A Binding Protein

CONFORMATIONAL SENSITIVITY TO LONG CHAIN FATTY ACYL-CoA*

(Received for publication, December 8, 1997, and in revised form, February 9, 1998)

Andrey Frolov and Friedhelm Schroeder‡

From the Department of Physiology and Pharmacology, Texas A & M University, TVMC, College Station, Texas 77843-4466

Cellular unbound long chain fatty acyl-CoAs (>14 carbon) are potent regulators of gene transcription and intracellular signaling. Although the cytosolic acyl-CoA binding protein (ACBP) has high affinity for medium chain fatty acyl-CoAs, direct interaction of ACBP with >14-carbon fatty acyl-CoAs has not been established. Steady state, photon counting fluorescence spectroscopy directly established that rat liver ACBP bound 18-carbon *cis*- and *trans*-parinaroyl-CoA, K_d = 7.03 ± 0.95 and 4.40 ± 0.43 nM. Time-resolved fluorometry revealed that ACBP-bound parinaroyl-CoAs had high rotational freedom within the single, relatively hydrophobic (ϵ <32), binding site. Tyr and Trp fluorescence dynamics demonstrated that apo-ACBP was an ellipsoidal protein (axes of 15 and 9 Å) whose conformation was altered by oleoyl-CoA in the holo-ACBP as shown by a 2-Å decrease of ACBP hydrodynamic diameter and increased Trp segmental motions. Thus, native liver ACBP binds >14-carbon fatty acyl-CoAs with nanomolar affinity at a single binding site. Acyl-CoA-induced conformational alterations in ACBP may be significant to its putative functions in lipid metabolism and regulation of processes sensitive to unbound long chain fatty acyl-CoAs.

It is now recognized that long chain fatty acyl-CoAs (>14 carbons) serve at least four essential cellular functions as follows: fatty acid oxidation (1–7), fatty acid esterification (8–16), signal transduction (17–19), and gene expression (20, 21). Although cellular long chain fatty acyl levels are normally in the range 5–164 μM, these levels increase as much as 4-fold in pathological conditions (reviewed in Ref. 22). Since the critical micellar concentration of long chain fatty acyl-CoAs is 30–60 μM and as much as 96–99% of long chain fatty acyl-CoA partitions to membranes, this suggests that high levels of long chain fatty acyl-CoAs may disrupt membrane function as well as cellular signaling/gene regulation (reviewed in Refs. 10 and 22).

Because of these considerations, it is important to understand the mechanisms that regulate the distribution of intracellular free long chain fatty acyl-CoAs. One candidate cytosolic protein that may serve this purpose is ACBP[1] which may sequester, store, and/or protect fatty acyl-CoAs from hydrolysis (reviewed in Ref. 22). Acyl-CoA binding protein (ACBP) is a small (10 kDa), highly conserved cytosolic protein broadly distributed among all eukaryotic tissues studied, and elevated expression of ACBP has been observed in malignant tumors and transformed cells (reviewed in Refs. 22–24).

A primary objective of the present investigation was to use a fluorescent fatty acyl-CoA binding assay as well as non-fluorescent oleoyl/acyl-CoA to directly show for the first time that native rat liver ACBP actually bound the most common chain length, C_{18}, fatty acyl-CoAs. The second aim was to examine the structural dynamics of native rat liver apo- and holo-ACBP, to characterize the properties of fluorescent fatty acyl-CoAs within the ACBP-binding site, and to examine ACBP conformational dynamics in response to ligand binding.

EXPERIMENTAL PROCEDURES

Materials

cis- and *trans*-parinaroyl-CoAs were synthesized as described (9). *cis*- and *trans*-parinaric acids were from Calbiochem. Coenzyme A (CoASH), acyl-coenzyme A synthase, ATP, *p*-terphenyl, and 1,4-bis[4-methyl-5-phenyl-2-oxazolyl]benzene, and saturated and unsaturated fatty acyl-CoAs were from Sigma. All other chemicals were reagent grade or better.

Methods

ACBP was isolated from rat liver as described previously (24). Protein concentration was determined by the Bradford assay (25) and corrected according to UV spectrophotometric analysis (26). The Bradford assay overestimates ACBP concentration by 1.69-fold.

Steady State Fluorescence Spectroscopy

Steady state fluorescence spectra were measured in a 1-cm quartz cuvette with a PC1 Photon Counting Spectrofluorimeter (ISS Instr., Champaign, IL). Sample temperature was maintained at 25 °C (±0.1 °C). Excitation and emission bandwidths were 4 and 8 nm. Sample absorbance at the excitation wavelengths was ≤0.05.

Time-resolved Fluorescence Spectroscopy

Data Acquisition—All measurements of lifetime, differential polarized phase (limiting anisotropy, rotational rate), hydrodynamic radius, and wobbling in a cone angle were performed as described earlier with a GREG 250 Subnanosecond Multifrequency Cross-correlation and Modulation fluorometer with KOALA automatic sample compartment (ISS Instruments, Champaign, IL) (27–29). Intrinsic ACBP aromatic amino acids were excited with an Innova-Sabre argon ion laser (Coherent Laser Group, Palo Alto, CA) with automatic wavelength selection at λ = 275.4, 300.2, 302.4, and 305.5 nm (power output 340, 630, 800 and 460 milliwatts, respectively). ACBP intrinsic fluorescence was observed through 313 BP10 and 341 BP15 interference filters (Omega Optical Inc., Brattleboro, VT). The extrinsic fluorescent ligands, *cis*- and *trans*-parinaroyl-CoAs, were excited at 325 nm by a 424NB He-Cd laser (Liconix Inc., Sunnyvale, CA), and emission was observed through a KV389 low fluorescent cut-off filter (Schott Glass Technologies, Duryea, PA). Sample absorbance at the excitation wavelengths was ≤0.05. All data were obtained in 25 mM phosphate buffer, pH 7.4, at 25 °C.

Lifetime Data Analysis—Lifetime data were analyzed by ISS-187 Software (ISS Inc., Champaign, IL) as a sum of exponentials shown

* This work was supported in part by USPHS Grant DK41402 from the National Institutes of Health. The costs of publication of this article were defrayed in part by the payment of page charges. This article must therefore be hereby marked "*advertisement*" in accordance with 18 U.S.C. Section 1734 solely to indicate this fact.

‡ To whom correspondence should be addressed: Dept. of Physiology and Pharmacology, Texas A & M University, TVMC, College Station, TX 77843-4466. Tel.: 409-862-1433; Fax: 409-862-4929; E-mail: fschroeder@cvm.tamu.edu.

[1] The abbreviations used are: ACBP, acyl-CoA binding protein; L-FABP, liver fatty acid binding protein; SCP-2, sterol carrier protein-2; I-FABP, intestinal fatty acid binding protein; CoASH, coenzyme A, 9*Z*,11*E*,13*E*,15*Z*-octadecatetraenoyl coenzyme A, *cis*-parinaroyl-CoA.

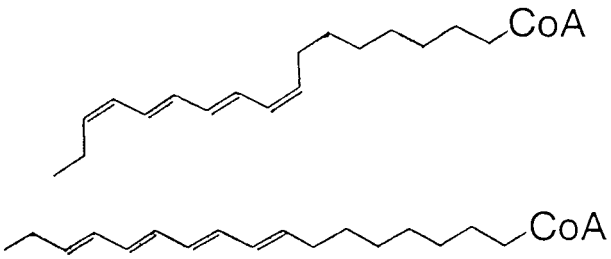

FIG. 1. **Chemical structures of 18-carbon fatty acyl-CoAs.** *cis-* and *trans*-parinaroyl-CoAs, *top* and *bottom*, respectively.

in Equation 1.

$$I(t) = \Sigma\alpha_i \exp(-t/\tau_I) \quad (1)$$

where I is fluorescence, τ_I is lifetime, and $\Sigma\alpha_i = 1$. Fractional intensity, f_i, was $f_i = \alpha_i\tau_I/\Sigma\alpha_i\tau_I$. Mean lifetime was $\Sigma f_i\tau_I$. The minimized χ^2 parameter was the criterion for goodness of fit to the model with $\chi^2 < 3$ acceptable (30).

Anisotropy Decay Data Analysis—Anisotropy decay was modeled by a sum of exponentials as follows: $r(t) = r(0)\Sigma g_i \exp(-t/\theta_i)$, where $r(0)$ is anisotropy of a fluorophore in the absence of rotational diffusion, θ_i is the rotational correlation time, and g_i is fractional anisotropy. The "goodness" of fit to the applied model was determined as described above using ISS-187 Software (ISS Instruments, Champaign, IL). The equivalent hydrodynamic radius of the protein was calculated as shown in Equation 2.

$$R = (3kT\theta/4\pi\eta)^{1/3} \quad (2)$$

where η is solvent viscosity. The value of the same parameter can be estimated from the hydrated protein volume as shown in Equation 3.

$$R = [(3/4\pi)(M/N_0)(V_2 + \delta_1 V_1)]^{1/3} \quad (3)$$

where M is molecular weight; N_0 is Avogadro's number; δ_1 is fraction of hydration; V_1 is volume of bound water; V_2 is protein-specific partial volume. δ_1 = 0.4 g H_2O/g protein; V_2 = 0.72 $cm^{-3}g^{-1}$ for an average protein (31), and V_1 = 1 cm^3g^{-1} for water in Equation 3.

Fluorescent Fatty Acyl-CoA Binding Assay

ACBP binding affinities for parinaroyl-CoAs were determined as described previously (28, 32) with the following modifications. A 2-ml sample of 0.05 μM ACBP in phosphate buffer was titrated with small increments of fatty acyl-CoA (0.1–1.0 μl) dissolved in double-distilled water. The fatty acyl-CoA stock solution concentrations were 270–300 μM. Each sample and blank (without ACBP) were thoroughly mixed and allowed to equilibrate for 1–2 min to permit stable measurement of the fluorescence signal. All measurements were performed at 25 °C.

RESULTS

Fluorescent Fatty Acyl-CoA Binding to Native Rat Liver ACBP

The binding affinity of native rat liver ACBP for fatty acyl-CoA was examined using a direct binding assay. This assay takes advantage of CoA derivatives of naturally occurring fluorescent parinaric acids and does not require separation of bound from free fatty acyl-CoA. As shown in Fig. 1, *cis-* and *trans*-parinaroyl-CoA are both 18-carbon fatty acids with 4 conjugated double bonds near the methyl terminus of the fatty acyl chain. *cis*-Parinaroyl-CoA has a *cis*-double bond at position 9, the same as that of the 18-carbon oleoyl-CoA (Fig. 1). Consequently, the kinked shape of the *cis*-parinaroyl-CoA acyl chain is nearly superimposable on that of the oleoyl-CoA acyl chain. In contrast, *trans*-parinaroyl-CoA has a straight chain fatty acyl chain, just like that of the 18-carbon stearoyl-CoA acyl chain (Fig. 1). Consequently, the straight shape of the *trans*-parinaroyl-CoA acyl chain is nearly superimposable on that of the stearoyl-CoA acyl chain. These properties make *cis-* and *trans*-parinaroyl-CoA excellent fluorescent structural analogues oleoyl- and stearoyl-CoA, respectively.

Although *cis-* and *trans*-parinaroyl derivatives fluoresce poorly in aqueous solution, upon titration of ACBP with *cis-* or *trans*-parinaroyl-CoA the fluorescence intensity increased, consistent with the ligand becoming localized in a more hydrophobic environment, *i.e.* protein binding pocket (Fig. 2). No shifts of *cis-* or *trans*-parinaroyl-CoA fluorescence emission maxima were detected upon titration of ACBP (data not shown). Therefore, the increase in fluorescence emission intensity of the parinaroyl-CoAs, measured at 420 nm after each addition of ligand to ACBP, was corrected for the background (no protein) and plotted as a function of total ligand concentration. This procedure yielded pure saturation curves for both *cis-* and *trans*-parinaroyl-CoA as shown in Fig. 2, *A* and *B*, respectively. Maximal fluorescence intensities were determined by titrating a small amount of each parinaroyl-CoA with increasing ACBP. These data were then used to construct Scatchard plots (Fig. 2, *A* and *B, insets*) and obtain binding parameters, dissociation constant (K_d), and molar stoichiometry (B_{max}). Native rat liver ACBP bound *cis-* and *trans*-parinaroyl-CoAs at a single binding site: *cis*-parinaroyl-CoA B_{max} = 0.93 ± 0.04 mol/mol, *trans*-parinaroyl-CoA B_{max} = 0.89 ± 0.01 mol/mol. The respective

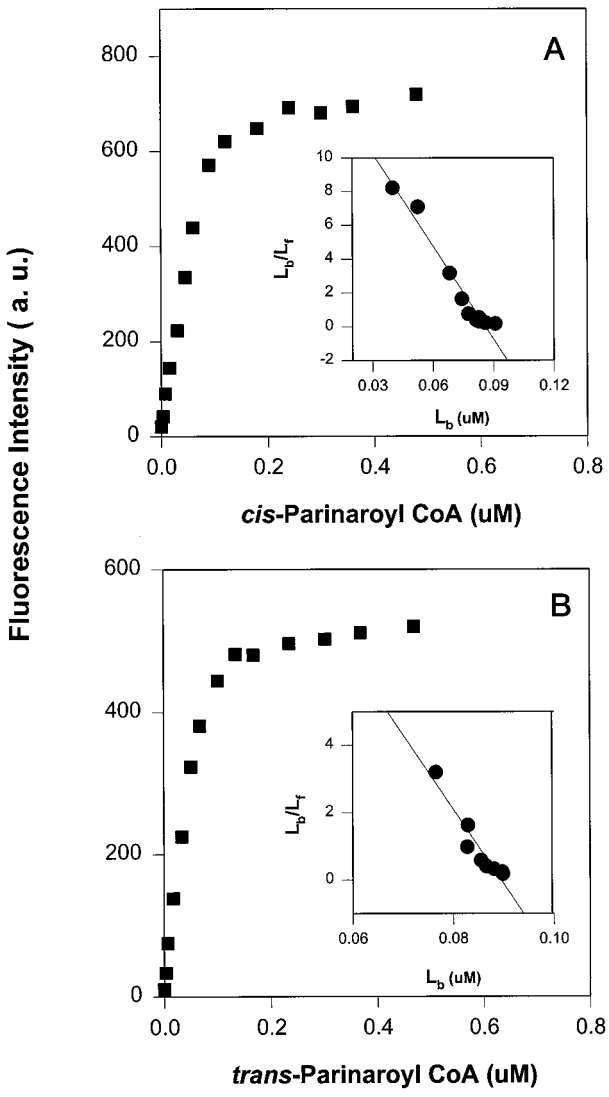

FIG. 2. **Titration of ACBP with parinaroyl-CoAs.** *A*, titration of ACBP (0.1 μM) with *cis*-parinaroyl-CoA (0–0.6 μM) as followed by the increase in fluorescence intensity. Excitation was at 310 and emission was at 416 nm. *Inset*, Scatchard plot of the titration of ACBP with *cis*-parinaroyl-CoA. *B*, titration of ACBP (0.1 μM) with *trans*-parinaroyl-CoA (0–0.6 μM). λ_{ex} = 310 and λ_{em} = 416 nm. *Inset*, Scatchard plot of the titration of ACBP with *trans*-parinaroyl-CoA. *a.u.,* absorbance units.

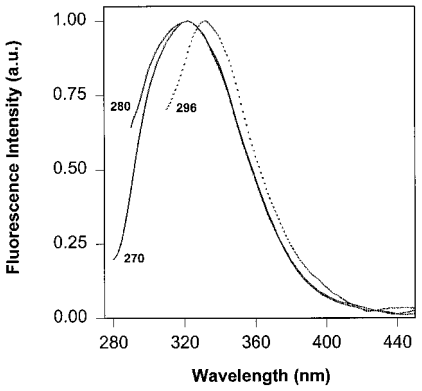

FIG. 3. **Fluorescence emission spectra of ACBP.** Spectra were normalized and corrected for the emission monochromator. The *numbers* next to the curves indicate the excitation wavelengths. Spectra were obtained with 1 μM ACBP in phosphate buffer, pH 7.4, at 25 °C.

affinities were K_d = 7.03 ± 0.95 and 4.4 ± 0.43 nM. The binding affinity of ACBP for the straight chain *trans*-parinaroyl-CoA was significantly 1.5-fold higher than that for the kinked chain *cis*-parinaroyl-CoA. In summary, these data provide the first direct evidence that ACBP binds naturally occurring 18-carbon chain fatty acyl-CoAs with nanomolar affinity.

Steady State Fluorescence Properties of Native Rat Liver Apo-ACBP

Rat liver ACBP is a protein with multiple intrinsic fluorophores, four Tyr and two Trp amino acid residues (24), which may result in a heterogeneous fluorescence emission of ACBP. Indeed, upon excitation at 270 nm, the wavelength where both Tyr and Trp were excited, native rat liver apo-ACBP had a rather broad (bandwidth 65 nm) fluorescence emission spectrum with a maximum at 322 nm and a shoulder near 300 nm (Fig. 3). Shifting the excitation wavelength to 280 nm resulted in a 7-nm (bandwidth 72 nm) broadening of the emission spectrum, almost exclusively on its blue edge. However, there was no effect on the position of the emission maximum (λ_{max} = 322 nm) (Fig. 3). Further shifting the excitation wavelength to 296 nm, the wavelength where Trp residues were preferentially selectively excited, the apo-ACBP emission maximum (λ_{max} = 332 nm) underwent a dramatic (~10 nm) bathochromic shift, and the emission spectrum was narrowed by almost 11 nm (bandwidth 61 nm), as compared with that of excitation at 280 nm (Fig. 3).

In summary, the fluorescence emission characteristics of apo-ACBP proved to be strongly dependent on excitation wavelength. The data showed that apo-ACBP fluorescence spectra had a distinct Tyr emission component as evidenced by an unusually short wavelength emission maxima (λ_{max} = 322 nm) upon excitation at 270 and 280 nm, as well as by the appearance of a characteristic Tyr emission shoulder near 300 nm upon excitation at 270 nm. Concomitantly, the apo-ACBP Trp emission component was clearly identified by its emission maximum at 332 nm upon excitation at 296 nm. The fact that native rat liver apo-ACBP had rather broad emission spectra (bandwidth 60–70 nm), regardless of the excitation wavelength (270–296 nm), was also consistent with both Tyr(s) and Trp(s) being present in highly heterogenous loci within the ACBP protein. In the case of the apo-ACBP Trp residues, these loci were characterized as highly hydrophobic, as shown by the fluorescence emission maximum of 332 nm (excitation at 296 nm) (33).

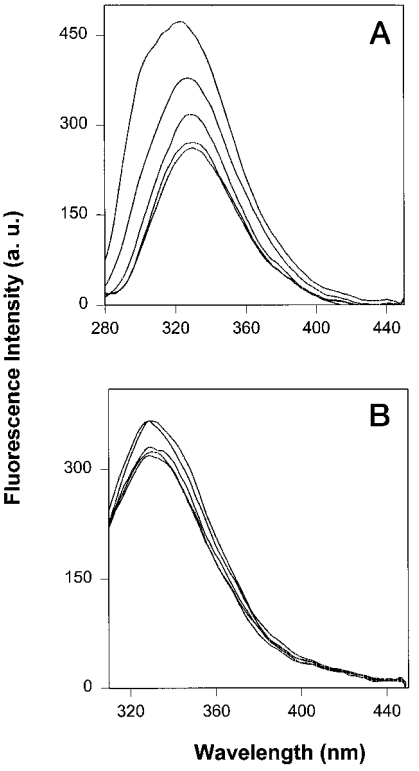

FIG. 4. **Fluorescence emission spectra of apo- and holo-ACBP.** Fluorescence emission spectra of ACBP (1 μM) were determined with and without oleoyl-CoA from *top* to *bottom*: no, 0.69 μM, 1.38 μM, 5.52 μM, 9.66 μM oleoyl-CoA. *A*, excitation at 270 nm. *B*, excitation at 296 nm.

Effect of Oleoyl-CoA Binding on Steady State Fluorescence Characteristics of Native Rat Liver ACBP

The effect of oleoyl-CoA binding on fluorescence emission characteristics of native rat liver ACBP aromatic amino acid residues was monitored by exciting the protein emission at two wavelengths, 270 and 296 nm. The excitation at 270 nm resulted in emission from both Tyr and Trp components, whereas the 296-nm excitation allowed observation primarily of ACBP Trp emission (see above). As shown in Fig. 4*A*, upon excitation at 270 nm, the fluorescence emission of ACBP was progressively quenched (up to 2-fold) upon titration apo-ACBP with increasing amounts of non-fluorescent oleoyl-CoA to form holo-ACBP. The reduction in fluorescence intensity was accompanied by a gradual red shift of the ACBP emission maximum (Fig. 4*A*). The latter shifted almost 8 nm (from 322 to 330 nm), when oleoyl-CoA was present in 10-fold molar excess over ACBP (Fig. 4*A*). The disappearance of both the shoulder observed near 300 nm in the ACBP emission spectrum (Fig. 4*A*) and the gradual spectral shift of the emission maximum to the position of the Trp emission maximum (λ_{max} = 330 nm, see Figs. 3 and 4*A*) were consistent with oleoyl-CoA predominantly quenching the Tyr fluorescence emission component of ACBP. This suggestion was further supported by results of experiments where the same titration was repeated with excitation at 296 nm where Trp, rather than Tyr, was selectively excited (Fig. 4*B*). In contrast to titration with oleoyl-CoA and 270-nm excitation (Fig. 4*A*), ACBP fluorescence emission and the position of its maximum (λ_{max} = 332 nm) were not significantly changed by oleoyl-CoA binding (Fig. 4*B*) when the ACBP was excited at 296 nm. Thus, ACBP Trp residues did not appear available for quenching induced by the bound oleoyl-CoA. In summary, the differential effects of oleoyl-CoA on ACBP Tyr and Trp fluorescence emission characteristics were consistent

TABLE I
Fluorescence decay of ACBP

Fluorescence decay was analyzed as a sum of exponentials: $I(t) = \Sigma\alpha_i \exp(-t/\tau_i)$ and one of the lifetime component was set fixed to 0.001 ns (not shown) in order to mimic an input of the light scatter. The fraction of the light scatter for all samples was ≤0.08. All measurements were made in phosphate-buffered saline, pH 7.4 at 25 °C.

Excitation/ emission	Sample	τ_1	τ_2	f_1	f_2	$\langle\tau\rangle^a$
		ns				*ns*
275/313	ACBP	2.44 ± 0.18	0.76 ± 0.08	0.18 ± 0.03	0.82 ± 0.03	1.06 ± 0.03
	ACBP/oleoyl-CoA	0.79 ± 0.02	0.18 ± 0.00	0.68 ± 0.001	0.32 ± 0.001	0.59 ± 0.01
275/341	ACBP	1.51 ± 0.11	0.53 ± 0.02	0.48 ± 0.03	0.52 ± 0.03	0.99 ± 0.03
	ACBP/oleoyl-CoA	1.35 ± 0.06	0.37 ± 0.03	0.51 ± 0.02	0.49 ± 0.02	0.86 ± 0.04
300/341	ACBP	1.15 ± 0.06	0.34 ± 0.001	0.52 ± 0.002	0.48 ± 0.002	0.76 ± 0.02
	ACBP/oleoyl-CoA	1.11 ± 0.03	0.24 ± 0.01	0.51 ± 0.01	0.49 ± 0.01	0.69 ± 0.01

[a] Average fluorescence lifetime $\langle\tau\rangle$ was calculated as $\langle\tau\rangle = \Sigma f_i\tau_i$.

with the following: (i) ACBP Tyr, but not Trp, residue(s) being localized within the oleoyl-CoA binding pocket, and/or (ii) ligand-induced conformational changes in the ACBP tertiary structure. These possibilities were resolved in the following sections.

Time-resolved Fluorescence

Fluorescence Lifetime of Apo- and Holo-ACBP—Time-resolved fluorescence studies of apo- and holo-ACBP were performed to understand better the nature of ACBP emission as well as the processes occurring in the protein globule on the pico- to nanosecond time scale upon ligand binding. The fluorescence decay of apo-ACBP was biexponential in nature, consistent with the presence of several emitting centers in the protein. Upon exciting at 275 nm (both Tyr and Trp excitation) but measuring emission at 313 nm (*i.e.* preferential measurement of ACBP Tyr emission at the blue edge of ACBP emission spectrum, Fig. 3), the major lifetime component was τ_1 = 0.76 ns (fraction 0.82), and the minor component was τ_2 = 2.44 ns (Table I). This biexponential decay resulted in a mean lifetime of $\langle\tau\rangle$ = 1.06 ns (Table I). Addition of 10 molar eq of oleoyl-CoA to form the holo-ACBP reduced both the long lifetime value, from 2.44 to 0.79 ns, and even more dramatically the short component from 0.76 to 0.18 ns, while increasing the fraction of the long lifetime component by almost 4-fold, from 0.18 to 0.68. The overall effect of oleoyl-CoA binding to ACBP was a reduction of the average lifetime by approximately 2-fold, from 1.06 to 0.59 ns (Table I).

When ACBP was excited at 275 nm (both Tyr and Trp excitation) but emission was observed at 341 nm (*i.e.* preferential measurement of ACBP Trp emission on the red edge of ACBP emission spectrum, Fig. 3), the biexponential decay displayed different characteristics as compared with conditions favoring excitation and emission of ACBP Tyr (*e.g.* 275/313 nm excitation/emission). The long lifetime component was τ_1 = 1.51 ns (fraction 0.48), and the short component was τ_2 = 0.53 ns (Table I). However, the average lifetime $\langle\tau\rangle$ = 0.99 ns (Table I) upon preferential excitation/emission of Trp was essentially the same as that upon preferential excitation/emission of ACBP Tyr. In contrast to preferential Tyr excitation/emission of ACBP, addition of 10 molar eq of oleoyl-CoA exerted a much smaller effect on fluorescence decay of the ACBP Trp. The main alteration detected was an ~30% reduction of the short lifetime component from 0.53 to 0.37 ns (Table I). The long lifetime component and its fraction, 1.35 ns and 0.51, respectively, remained almost unchanged (Table I). Consequently, the average lifetime appeared to decline only slightly but was not statistically significant from 0.99 to 0.86 ns (Table I).

In contrast to excitation at 275 nm, excitation of ACBP at 300 nm (partial selective excitation of ACBP Trp) and measurement of fluorescence emission at 341 nm (partial selective ACBP Trp emission) minimized contributions from the ACBP Tyr component while maximizing contributions from the ACBP Trp component (Fig. 3). Under the ACBP Trp partial selective excitation/emission conditions, 300/341 nm, ACBP fluorescence decay exhibited long, τ_1 = 1.15 ns, and short, τ_2 = 0.34 ns, lifetime components with the respective fractions being 0.52 and 0.48 (Table I). The average lifetime was calculated to be $\langle\tau\rangle$ = 0.76 ns (Table I). When 10 molar eq of oleoyl-CoA was added to the ACBP, no dramatic changes in the parameters of ACBP fluorescence decay were observed (Table I).

In summary, similar to the steady state fluorescence characteristics (Fig. 3), the native rat liver ACBP fluorescence lifetime parameters also appeared to be wavelength dependent (Table I), reflecting the contributions of both Tyr and Trp to ACBP emission. The major alteration in ACBP fluorescence decay upon oleoyl-CoA binding to the protein, ~2-fold reduction in the average lifetime, was observed under conditions preferentially monitoring ACBP Tyr (275/313 nm excitation/emission) (Table I). The fact that ACBP fluorescence intensity was also reduced by ~2-fold after addition of 10 molar eq of oleoyl-CoA (Fig. 4*A*) was consistent with the mechanism of ACBP fluorescence quenching by oleoyl-CoA being predominantly dynamic in nature.

Anisotropy of Apo- and Holo ACBP—Time-resolved fluorescence anisotropy was used to examine the rotational dynamics of native rat liver apo-ACBP Tyr. Upon excitation at 275 nm and measurement of fluorescence emission at 313 nm, ACBP exhibited monoexponential anisotropy decay kinetics with a rotational correlation time θ = 3.07 ns (Table II). This relatively long correlation time reflected overall protein motion and was consistent with that expected for protein (ACBP) with molecular mass near 10 kDa (31). The ACBP hydrodynamic radius calculated from the time-resolved anisotropy data was 15.1 Å (Table II). The fact that the measured residual (limiting) anisotropy of ACBP r = 0.156 (Table II) was much less than both the maximal Trp and Tyr anisotropies measured in a propylene glycol glass at −60 °C, r_0 = 0.315 (34), and r_0 = 0.320 (35), respectively, indicates that ACBP aromatic amino acid local segmental motions were relatively fast and not resolvable on the nanosecond time scale. In addition to this fast rotation, the estimated amplitude for such rotational motions, *i.e.* the "wobbling" in cone angle, was also large, near 36° (Table II).

The effect of ligand binding on the rotational dynamics of native rat liver ACBP Tyr was examined. Addition of 10-fold eq of oleoyl-CoA did not affect the monoexponentiality of ACBP anisotropy decay but significantly decreased the protein rotational correlation time from 3.07 to 2.1 ns (Table II). This

TABLE II
Anisotropy decay of ACBP
The anisotropy of ACBP was analyzed by a sum of exponentials as $r(t) = r_0 \Sigma g_i \exp(-t/\theta_i)$.

Excitation/ emission	Sample	θ	r^a	Radius	Wobbling cone angle, degree[b]
		ns		*Å*	
275/313	ACBP	3.07 ± 0.10	0.156 ± 0.008	15.1	36
	ACBP/oleoyl-CoA	2.10 ± 0.12	0.163 ± 0.007	13.3	35
275/341	ACBP	3.11 ± 0.08	0.114 ± 0.002	15.1	41
	ACBP/oleoyl-CoA	2.44 ± 0.11	0.124 ± 0.009	14.0	40
300/341	ACBP	0.76 ± 0.06	0.320 ± 0.007	9.5	
	ACBP/oleoyl-CoA	0.54[a] ± 0.02	0.312 ± 0.006	8.5	7

[a] r was allowed to vary.
[b] The wobbling cone angle was calculated from time-resolved fluorescence anisotropy data using the following equation: $r/r_0 = (3\cos^2\phi - 1)/2$, where r is the residual (limiting) anisotropy and r_0 is the maximal fluorescence anisotropy, or the anisotropy at the zero time. r_0 value was assumed as 0.32, the fundamental Trp and Tyr anisotropy in propylene glycol at −60 °C (34, 35).

reduction in ACBP rotational correlation time corresponded to a decrease in the protein hydrodynamic radius, from 15.1 to 13.3 A (Table II). Despite this alteration in ACBP hydrodynamic radius, the amplitude of the segmental mobility of ACBP aromatic amino acids was not significantly changed as indicated by a wobbling in a cone angle of $\phi = 35°$ (Table II).

The 275 nm excitation and fluorescence detection on the red edge of ACBP emission spectrum (λ=341 nm) also revealed mono-exponential decay of ACBP anisotropy and a rotational rate, $\theta = 3.11$ ns, similar to that obtained under conditions favoring ACBP Tyr emission (275/313 nm excitation/emission) (Table II). However, the much lower value of protein limiting anisotropy in this case, $r = 0.114$ *versus* 0.156 (Table II), resulted in higher amplitude for the internal motions of ACBP aromatic amino acid residues, $\phi = 41°$ (Table II). Addition of 10-fold molar eq of oleoyl-CoA significantly decreased the overall rotational correlation time from 3.11 to 2.44 ns, increased the limiting anisotropy from 0.114 to 0.124, and decreased the calculated wobbling in cone angle slightly from 41 to 40° (Table II).

Upon excitation at 300 nm, ACBP emission at 341 nm exhibited dramatically different anisotropy decay characteristics. As shown in Table II, ACBP showed very fast single rotational correlation time, $\theta = 0.76$ ns, and a high limiting anisotropy $r = 0.320$. This high limiting anisotropy was similar to the maximal Trp and Tyr anisotropies measured in propylene glycol glass at −60 °C (34, 35). The latter results were consistent with the internal motions of the protein amino acid residues responsible for the observed fluorescence being completely restricted on the nanosecond time scale. The calculated respective protein hydrodynamic radius, based on selective ACBP Trp emission, was 9.5 Å (Table II), much lower than that of ~15 Å estimated from ACBP fluorescence parameters favoring ACBP Tyr (*e.g.* 275/313 nm excitation/emission) conditions (Table II).

Time-resolved Fluorescence of cis- and trans-Parinaroyl-CoAs in the ACBP Fatty Acyl-CoA-binding Site—The molecular dynamics of the fatty acyl-CoA ligand within the ACBP-binding site were examined. *cis*- and *trans*-parinaroyl-CoA were bound to ACBP, and their fluorescence intensity and anisotropy decays were determined.

Fluorescence Lifetime—As shown in Table III, ACBP bound *cis*- and *trans*-parinaroyl-CoAs both displayed complex fluorescence decay kinetics which were best fit ($\chi^2 < 3$) to three exponentials. The absolute values of the longest fluorescence decay components τ_1 ~70 ns presented in Table III must be considered as their lowest limit. The best fits ($\chi^2 < 3$) of the respective emission kinetics yielded a range of values, 70–500 ns, for this slowest component of the different emission decay curves, without changing the other components and their respective fractions (data not shown). The calculated average lifetimes for *cis*- and *trans*-parinaroyl-CoA bound to ACBP were 10.55 and 7.38 ns, respectively (Table III). These average lifetime values were significantly longer than that of *cis*-parinaroyl-CoA in ethanol, $<\tau> = 4.5$ ns (27). These observations were consistent with the fluorophore (tetraene located between C_{10} to C_{18} of the fatty acyl chain) of *cis*- and *trans*-parinaroyl-CoA being rather shielded from the aqueous solution when bound to ACBP. Furthermore, the longer average lifetime of *cis*-parinaroyl-CoA bound to ACBP also suggested that the *cis*-parinaroyl-CoA was localized in a more hydrophobic and/or restricted microenvironment as compared with the *trans*-parinaroyl-CoA (shorter average lifetime).

Fluorescence Anisotropy—The analysis of anisotropy decay of *cis*- and *trans*-parinaroyl-CoAs bound to ACBP revealed single exponential kinetics for both ligands. Both molecules exhibited similar rotational correlation times, $\theta = 3.30$ and 3.37 ns, respectively, within the ACBP fatty acyl-CoA-binding site (Table IV). It should be noted that the rotational correlation time values observed for parinaroyl-CoAs bound to ACBP were nearly identical to those obtained for ACBP protein overall rotations, based on the intrinsic ACBP fluorescence upon excitation at 275 nm (Table II). Therefore, the rotational correlation times measured for the bound parinaroyl-CoAs (Table IV) can be assigned to the rotational motions of the holo-ACBP. The respective hydrodynamic radii for ACBP bearing *cis*- or *trans*-parinaroyl-CoAs were calculated to be ~15.5 and 15.6 Å (Table IV).

A fast rotational component, due to segmental motions of *cis*- or *trans*-parinaroyl-CoAs within the ACBP binding pocket (27), was not observed in the *cis*- or *trans*-parinaroyl-CoA fluorescence anisotropy decay kinetics. The absence of fast rotations for *cis*- or *trans*-parinaroyl-CoAs within the ACBP binding pocket can result from one of two effects. (i) Such motions were completely restricted because of sterical restraints imposed on the bound ligand by the ACBP globule. However, if this was a case, one might expect the respective measured maximal (limiting) anisotropy values for *cis*- or *trans*-parinaroyl-CoAs in the binding pocket, $r = 0.156$ and 0.187 (Table IV), to be close to those reported for *cis*- and *trans*-parinaric acid in propylene glycol glass, $r = 0.38$ and 0.39, respectively (36). (ii) The motions were very fast. The fact that the maximal anisotropy values of the *cis*-(*trans*)-parinaroyl-CoA bound to ACBP were only half of those expected for completely immobilized fluorophores was consistent with both *cis*- and *trans*-parinaroyl-CoAs undergoing very fast rotational depolarizing motions in the ACBP binding pocket not resolvable on the nanosecond time

TABLE III

Fluorescence decay of cis-(trans)-parinaroyl CoA bound to ACBP

The fluorescence of parinaroyl-CoAs was analyzed as described in the legend to Table I. All measurements were made in phosphate-buffered saline, pH 7.4, at 25 °C. PA, parinaroyl.

Sample	τ_1	τ_2	τ_3	f_1	f_2	f_3	$\langle\tau\rangle^a$
	ns	*ns*	*ns*				*ns*
cis-PA-CoA	>70	3.05 ± 0.08	0.91 ± 0.06	0.13 ± 0.01	0.20 ± 0.02	0.67 ± 0.01	10.55 ± 0.92
trans-PA-CoA	>70	1.86 ± 0.14	0.59 ± 0.02	0.09 ± 0.003	0.25 ± 0.02	0.66 ± 0.02	7.38 ± 0.23

[a] Average fluorescence lifetime $\langle\tau\rangle$ was calculated as $\langle\tau\rangle = \Sigma f_i\tau_i$.

TABLE IV

Anisotropy decay of cis- and trans-parinaroyl-CoA bound to ACBP

The anisotropy of parinaroyl-CoAs (PA-CoA) was analyzed by a sum of exponentials as $r(t) = r_0\Sigma g_i\exp(-t/\theta_i)$.

Sample	θ (ns)	r^a	Radius	Wobbling cone angle, degree[b]
			Å	
cis-PA-CoA	3.30 ± 0.15	0.156 ± 0.006	15.5	39
trans-PA-CoA	3.37 ± 0.12	0.187 ± 0.004	15.6	36

[a] r was allowed to vary.

[b] The wobbling cone angle was calculated on the basis of time-resolved fluorescence anisotropy data presented in the table and by using the following equation: $r/r_0 = (3\cos^2\phi - 1)/2$, where r is the residual (limiting) anisotropy and r_0 is the maximal fluorescence anisotropy, or the anisotropy at the zero time. r_0 value was assumed to be 0.38 and 0.39 for *cis*- and *trans*-parinaroyl-CoA, respectively, the same as measured for *cis*- and *trans*-parinaric acid in propylene glycol at −60 °C (36).

scale. The estimated amplitude of *cis*- and *trans*-parinaroyl-CoA rotational motions was calculated to be 39 and 36°, respectively (Table IV). It appeared that kinked fatty acyl-CoA (*cis*-parinaroyl-CoA), as compared with its straight counterpart (*trans*-parinaroyl-CoA), had more rotational freedom in ACBP binding pocket.

DISCUSSION

Although the amino acid sequence of ACBP is relatively conserved among a variety of species, to date much of our knowledge of ACBP is limited to the bovine. Data from other fatty acyl-CoA binding protein families indicate that an alteration of even a single amino acid residue may dramatically alter its ligand specificity (37–39) and/or structure/function (reviewed in Refs. 27 and 39–41).

The present study used a direct binding assay to demonstrate for the first time that native rat ACBP binds the naturally most prevalent chain length (18 carbon) fatty acyl-CoAs with nanomolar affinity. This finding is especially significant since examination of fatty acyl-CoA binding affinities over the past several years focused largely on ≤16-carbon fatty acyl-CoAs binding to bovine ACBP. Moreover, the actual affinity of bovine ACBP for the most common naturally occurring long chain (>14 carbon) fatty acyl-CoAs is uncertain (22). Part of the problem lies in the lack of consistency of different fatty acyl-CoA binding assays which have yielded K_d values ranging from 10^{-6} to 10^{-14} M. Furthermore, even state of the art binding assays such as microcalorimetry could not provide a direct binding assay for >14-carbon fatty acyl-CoAs, whereas an indirect (displacement) microcalorimetry binding assay required a number of assumptions to yield reasonable data for bovine ACBP and the 16-carbon hexadecanoyl-CoA, ranging nearly 5 orders of magnitude (22, 42). As shown herein, native rat liver ACBP had high affinity, nM K_d, for the naturally occurring C_{18} kinked (*cis*-parinaroyl-CoA) and C_{18} straight (*trans*-parinaroyl-CoA) acyl-CoAs: 7.03 and 4.4 nM, respectively. Consistent with this, an indirect microcalorimetric binding assay concluded that bovine ACBP bound C_{16} palmitoyl-CoA with a K_d = 2 nM (42) while another indirect binding assay (membrane partitioning/competition) yielded a K_d = 5 nM for bovine ACBP (10, 42). Additionally, analysis of *cis*-parinaroyl-CoA displacement data by a series of saturated and unsaturated acyl-CoAs with different chain lengths revealed that rat liver ACBP binds saturated fatty acyl-CoAs with chain lengths ranging from C_{12} to C_{20} and unsaturated fatty acyl-CoAs with chain length from C_{14} to C_{20}.[2]

The same fluorescent method and ligands were used to assess the binding affinities of ACBP, sterol carrier protein-2 (29) and liver fatty acid binding protein (39). This allows direct comparison of ACBP, SCP-2, and L-FABP long chain fatty acyl-CoA binding affinities. The binding K_d values of SCP-2 for *cis*- and *trans*-parinaroyl-CoA were reported to be 4.57 and 2.76 nM (29). The same parameters measured for the L-FABP high affinity binding site yielded 8 and 10 nM K_d values, as well as 97 and 180 nM K_d values for the L-FABP low affinity binding site (39). Thus, it appears that among these proteins SCP-2 had a slightly higher binding affinity for parinaroyl-CoAs, followed by ACBP and then by L-FABP. Interestingly, both ACBP and SCP-2 (but not L-FABP) exhibited a similar trend; they bound straight chain *trans*-parinaroyl-CoA tighter than the kinked chain counterpart. In summary, all three fatty acyl-CoA proteins would be expected to play a role in determining cellular fatty acyl-CoA partitioning between membranes and aqueous/cytosolic compartments, although the subcellular distribution of these proteins is quite dissimilar (22): ACBP is almost exclusively cytosolic; L-FABP is both cytosolic and associated with microsomes; SCP-2 is highly enriched (8-fold) in peroxisomes and less so (2-fold) in endoplasmic reticulum (43, 44). This suggests that ACBP, while not exclusively functioning in fatty acyl-CoA binding, may regulate fatty acyl-CoA function in different intracellular site(s).

The structural and dynamic data obtained using ACBP fluorescence characteristics in the present studies also provided several unique insights on the nature of this protein and its interaction with the most prevalent 18-carbon fatty acids.

First, ACBP appears unique among the cytosolic lipid binding proteins with regard to in its spectroscopic distribution of aromatic amino acid residues. Careful analysis revealed the presence of a strong Tyr emission component in ACBP emission spectra despite the presence of Trp residues in the protein. In contrast, no resolvable Tyr component was observed in emission spectra of another fatty acyl-CoA binding protein, intestinal fatty acid binding protein (I-FABP) (27), even though I-FABP, like ACBP, also contains four Tyr and two Trp amino acid residues. ACBP Tyr emission was observable because of

[2] T. H. Cho and F. Schroeder, unpublished observations.

the favorable conditions preventing excitation energy transfer within Tyr-Trp donor-acceptor pairs, internal Tyr fluorescence quenching by peptide bonds, hydrogen bond formation, or photochemical reactions in Tyr excited singlet state (45). These findings allowed resolution of new structure and molecular dynamics features of apo- and holo-ACBP.

Second, the above observations were used to show that the intrinsic Tyr fluorescence could be used to determine binding of the 18-carbon oleoyl-CoA to this protein. The mechanism of Tyr, but not Trp, fluorescence quenching upon oleoyl-CoA binding to ACBP was dynamic in nature as indicated by a perfect correlation between the level (~2-fold) of ACBP fluorescence decrease (Fig. 4*A*) and the decrease (~2-fold) of the average fluorescence lifetime value (275/313 excitation, Table II).

Third, ACBP Trp residues were at least partially spectroscopically resolvable and, along with bound ligand rotational data, were used to infer that native rat liver ACBP was ellipsoidal with semiaxes of 15 and 9 Å.

Fourth, the rotational dynamics of ACBP showed that ligand binding induced a significant change in tertiary structure of this protein as evidenced by the decrease of both short and long axis lengths by almost 2 Å. Interestingly, no alterations in ACBP secondary structure induced by the bound ligand were detectable by either circular dichroic spectra of rat ACBP[3] or by NMR spectroscopy of bovine recombinant ACBP (46). Similar observations of ligand-sensitive tertiary structure lability detectable by fluorescence techniques were also reported for other fatty acyl-CoA binding proteins, SCP-2 (29), L-FABP (27, 39), and I-FABP (27).

The role and significance of such protein conformational lability in protein-regulated lipid metabolic reactions, cell signaling (17–19), interactions with DNA/DNA binding proteins (20, 21), molecular recognition, or protein-protein interaction remain to be evaluated. In the latter cases, for example, it was recently shown that L-FABP isoforms possessing distinct secondary and tertiary structures (39) differentially modulated microsomal glycerol-3-phosphate acyltransferase and lysophosphatidic acyltransferase activities (41). Also, the holo-L-FABP isoform with bound fatty acid was a more potent stimulator of oleoyl-CoA incorporation into the phospholipids, as compared with its apo-form (41). Similar observations were made with another member of the fatty acid binding protein superfamily, the cellular retinol binding protein. The apo- and holo-forms of cellular retinol binding protein were selectively recognized by lecithin-retinol acyltransferase, resulting in differential modulation of enzyme activity (47).

In summary, the data presented new insights on the binding affinity, specificity, and potential function of ACBP in fatty acyl-CoA utilization. Furthermore, unique aspects of rat liver ACBP fluorescence emission allowed examination of the structural characteristics of apo- and holo-ACBP in solution, as well as the molecular dynamics of bound fatty acyl-CoA ligand measured in the nanosecond time range. This information significantly contributes to our understanding of ACBP structure and function(s) and can be used for a selective modification of ACBP functional activity by site-directed mutagenesis.

[3] A. Frolov and F. Schroeder, unpublished results.

REFERENCES

1. Shug, A. L., Lerner, E., Elson, C., and Shrago, E. (1971) *Biochem. Biophys. Res. Commun.* **43,** 557–563
2. Shug, A. L., Shrago, E., Bittar, N., Folts, J. D., and Koke, J. R. (1975) *Am. J. Physiol.* **228,** 689–692
3. Woldegiorgis, G., Shrago, E., Gipp, J., and Yatvin, M. (1981) *J. Biol. Chem.* **256,** 12297–12300
4. Tippett, P. S., and Neet, K. E. (1982) *J. Biol. Chem.* **257,** 12839–12845
5. Reddy, J. K., and Mannaerts, G. P. (1994) *Annu. Rev. Nutr.* **14,** 343–370
6. Wanders, R. J., Schutgens, R. B., and Barth, P. G. (1995) *J. Neuropathol. Exp. Neurol.* **54,** 726–739
7. Singh, I., Pahan, K., Singh, A. K., and Barbosa, E. (1993) *J. Lipid Res.* **34,** 1755–1764
8. Choy, P. C., and Arthur, G. (1990) in *Phosphatidylcholine Metabolism* (Choy, P. C., and Arthur, G., eds) pp. 87–101
9. Hubbell, T., Behnke, W. D., Woodford, J. K., and Schroeder, F. (1994) *Biochemistry* **33,** 3327–3334
10. Jolly, C. A., Hubbell, T., Behnke, W. D., and Schroeder, F. (1997) *Arch. Biochem. Biophys.* **341,** 112–121
11. MacDonald, J., and Sprecher, H. (1991) *Biochim. Biophys. Acta* **1084,** 105–121
12. Numa, S., and Yamashita, S. (1974) *Curr. Top. Cell. Regul.* **8,** 197–246
13. Lehrer, G., Panini, S. R., Rogers, D. H., and Rudney, H. (1981) *J. Biol. Chem.* **256,** 5612–5619
14. Jepson, C. A., and Yeaman, S. J. (1992) *FEBS Lett.* **310,** 197–200
15. Gavey, K. L., Noland, B. J., and Sallen, T. J. (1981) *J. Biol. Chem.* **256,** 2993–2999
16. Lands, W. F., and Hart, P. (1965) *J. Biol. Chem.* **240,** 1905–1911
17. Glick, B. S., and Rothman, J. E. (1987) *Nature* **326,** 309–312
18. Pfanner, N., Glick, B. S., Arden, S. R., and Rothman, J. E. (1990) *J. Cell Biol.* **110,** 955–961
19. Comerford, J. G., and Dawson, A. P. (1993) *Biochem. J.* **289,** 561–567
20. Brun, T., Assimacopoulos-Jeannet, F., Corkey, B. E., and Prentki, M. (1997) *Diabetes* **46,** 393–400
21. Li, Q., Yamamoto, N., Inoue, A., and Morisawa, S. (1990) *J. Biochem.* (*Tokyo*) **107,** 699–702
22. Gossett, R. E., Frolov, A. A., Roths, J. B., Behnke, W. D., Kier, A. B., and Schroeder, F. (1996) *Lipids* **31,** 895–918
23. Gossett, R. E., Schroeder, F., Gunn, J. M., and Kier, A. B. (1997) *Lipids* **32,** 577–585
24. Gossett, R. E., Edmondson, R. D., Jolly, C. A., Cho, T. H., Russell, D. H., Knudsen, J., Kier, A. B., and Schroeder, F. (1998) *Arch. Biochem. Biophys.* **350,** 201–213
25. Bradford, M. (1976) *Anal. Biochem.* **72,** 248–254
26. Pace, C. N., Vajdos, F., Fee, L., Grimsley, G., and Gray, T. (1997) *Protein Sci.* **4,** 2411–2423
27. Frolov, A. A., and Schroeder, F. (1997) *Biochemistry* **36,** 505–517
28. Stolowich, N. J., Frolov, A., Atshaves, B. P., Murphy, E., Jolly, C. A., Billheimer, J. T., Scott, A. I., and Schroeder, F. (1997) *Biochemistry* **36,** 1719–1729
29. Frolov, A., Cho, T. H., Billheimer, J. T., and Schroeder, F. (1996) *J. Biol. Chem.* **271,** 31878–31884
30. Parasassi, T., Conti, F., and Gratton, E. (1984) *Biochemistry* **23,** 5660–5664
31. Cantor, C. R., and Schimmel, P. R. (1980) *Biophysical Chemistry*, (Bartlett, A. C., Vapnek, P. C., and McCombs, L. W., eds) p. 554, W. H. Freeman & Co., San Francisco
32. Schroeder, F., Myers-Payne, S. C., Billheimer, J. T., and Wood, W. G. (1995) *Biochemistry* **34,** 11919–11927
33. Burstein, E. A., Vedenkina, N. S., and Ivkova, M. N. (1973) *Photochem. Photobiol.* **18,** 263–279
34. Lakowicz, J. R., Laczko, G., and Cherek, H. (1986) *J. Biol. Chem.* **261,** 2240–2245
35. Lakowicz, J. R., Laczko, G., and Gryczynski, I. (1987) *Biochemistry* **26,** 82–90
36. Wolber, P. K., and Hudson, B. S. (1981) *Biochemistry* **20,** 2800–2810
37. Jakoby, M. G., Miller, K. R., Joner, J. J., Bauman, A., Cheng, L., Li, E., and Cistola, D. P. (1993) *Biochemistry* **32,** 872–878
38. Sha, R. S., Kane, C. D., Xu, Z., Banaszak, L. J., and Bernlohr, D. A. (1993) *J. Biol. Chem.* **268,** 7885–7892
39. Frolov, A., Cho, T. H., Murphy, E. J., and Schroeder, F. (1997) *Biochemistry* **36,** 6545–6555
40. Schroeder, F., Jolly, C. A., Cho, T. H., and Frolov, A. A. (1998) *Chem. Phys. Lipids*, in press
41. Jolly, C. A., Murphy, E. J., and Schroeder, F. (1998) *Biochim. Biophys. Acta* **1390,** 258–268
42. Faergeman, N. J., and Knudsen, J. (1997) *Biochem. J.* **323,** 1–12
43. Krisans, S. K. (1996) *Ann. N.Y. Acad. Sci.* **804,** 142–164
44. Baum, C. L., Reschly, E. J., Gayen, A. K., Groh, M. E., and Schadick, K. (1997) *J. Biol. Chem.* **272,** 6490–6498
45. Demchenko, A. P. (1986) *Ultraviolet Spectroscopy of Proteins,* pp. 1–312, Springer-Verlag, Berlin, New York
46. Kragelund, B. B., Andersen, K. V., Madsen, J. C., Knudsen, J., and Poulsen, F. M. (1993) *J. Mol. Biol.* **230,** 1260–1277
47. Herr, F. M., and Ong, D. E. (1992) *Biochemistry* **31,** 6748–6755